

Electronic band structures and charge densities of NbC and NbN[†]

D. J. Chadi and Marvin L. Cohen

*Department of Physics, University of California, Berkeley, California 94720
and Inorganic Materials Research Division, Lawrence Berkeley Laboratory, Berkeley, California 94720*

(Received 3 December 1973)

We present nonlocal-pseudopotential calculations of the electronic band structures and charge densities of NbC and NbN. The major contribution to the charge density of the bands near the Fermi energy comes from C or N $2p$ states. The charge density for the first partially filled Nb $4d$ band and the shape of the Fermi surface for this band are also discussed.

I. INTRODUCTION

Transition-metal compounds have been the object of much research for some time because of their unusual physical properties. Some of these compounds are high-temperature superconductors with superconducting transition temperatures that vary appreciably with composition.¹ Despite the great practical and theoretical interest in these compounds, the electronic structure of many transition-metal compounds have not been studied in detail as yet.

In this paper we apply the empirical-pseudopotential method² (EPM) to the study of two transition-metal compounds: NbC and NbN. The band structure and density of states of NbN have been recently calculated by the augmented-plane-wave (APW)^{3,4} and the EPM⁵ methods. The band structure and density of states of NbN presented in this paper are the same as those of Ref. 5. For NbC only the density of states has been previously calculated using the APW method.⁶

Usual EPM calculations are based on experimental data such as optical reflectivity spectra, which provide information on critical-point energy gaps, and on photoemission data which give information on the density of states. Such experimental information is lacking for NbN and some other transition-metal compounds. The EPM band-structure calculation⁵ for NbN was therefore fitted to a self-consistent⁴ APW calculation. The results indicated that the nonlocal EPM method could be used for band-structure calculations of other transition-metal compounds of interest. In this paper we have extended the NbN calculation to NbC. Because of the lack of data this calculation is based on the use of Nb and C potentials derived from earlier EPM calculations. The lattice-constant change for C was large and the pseudopotential may not be accurate. The inaccuracy in the position of the lowest band in both NbC and NbN is also an indication that improvements are needed. This band is lower by almost 2 Ry compared to APW calculations.^{3,4} With these statements serving as a caveat, we have used the band-structure calculations to obtain the charge-

density distributions of the higher bands for both compounds. We find the band structures of NbC and NbN to be very similar to each other and, except for the lowest band, similar to Schwarz's calculation⁴ for NbN. The important difference between the two compounds appears to be the position of the Fermi energy which determines the occupancy and electronic charge distribution in the partially filled Nb $4d$ bands. The band structures, charge-density distributions, and Fermi surfaces of NbC and NbN are discussed in the Sec. II in more detail.

The pseudopotentials used in the NbC calculation were obtained from previous EPM calculations on NbN⁵ and C.⁷ The nonlocal d pseudopotential of the NbN calculation⁵ was used in NbC to treat the Nb $4d$ states. The nonlocal p pseudopotential needed for the C $2p$ states was obtained from a previous EPM calculation on C⁷ and adjusted for the lattice-constant change. All the relevant pseudopotential parameters for NbC are listed in Table I and their significance is discussed in Ref. 5 which

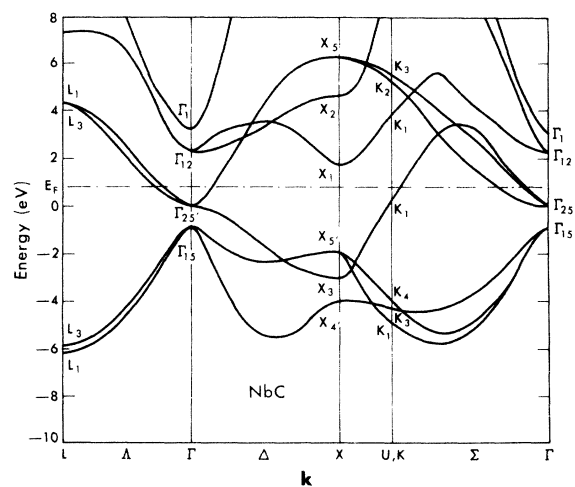


FIG. 1. Electronic energy band structure of NbC along principal symmetry directions. The lowest C $2s$ band is not shown. The zero of energy is at the Γ_{25} level.

TABLE I. Pseudopotential parameters for NbC. Nonlocal d and p pseudopotentials were used in addition to the local pseudopotentials in calculating the band structure of NbC.

Local pseudopotentials	Parameters for non-local d pseudopotential (see Ref. 5)	Parameters for non-local p pseudopotential (see Ref. 7)
$V^A(G^2=3) = 0.444$ Ry	$V_{nl} = \begin{cases} A_2, & r \leq R_s \\ 0, & r > R_s \end{cases}$	$V_{nl} = \begin{cases} A r e^{-\alpha r}, & r \leq R_s \\ 0, & r > R_s \end{cases}$
$V^A(11) = 0.06$ Ry	$R_s = 1.18$ Å	$R_s = 0.20$ Å
$V^S(4) = -0.14$ Ry	$A_2 = -4.65$ Ry	$A = -0.19$ Ry/Å
$V^S(8) = -0.11$ Ry	$\alpha = 0.118$	$\alpha = 1.10$ Å ⁻¹
$V^S(12) = -0.066$ Ry	$\kappa = 1.74$ ($2\pi/a$)	
$a = 4.47$ Å		

also includes the NbN pseudopotentials.

The energy band structure of NbC was calculated on a grid of 46 points in 1/48 of the irreducible part of the Brillouin zone. To obtain sufficient convergence for the charge-density calculation the wave functions for NbC and NbN were expanded in a basis set of about 150 plane waves. The band structure, charge density, and Fermi-surface results are discussed in Sec. II.

II. RESULTS

The band structures and densities of state of NbC and NbN are shown in Figs. 1–4. In discussing the band structures and charge densities of these compounds we will number the bands according to their energies. This can cause a band (such as band 3 in NbC and NbN) to be mostly p -like in some part of the Brillouin zone and d -like in another part of the zone, as can be seen by following band 3 from Γ to X . (Since the first band of NbC is not shown, band 3 in NbC refers to the second band shown in Fig. 1.)

The lowest band in NbC, as in NbN, is separated by a large energy difference from the higher bands. A nonlocal s -type pseudopotential is required to bring this band into better agreement with APW

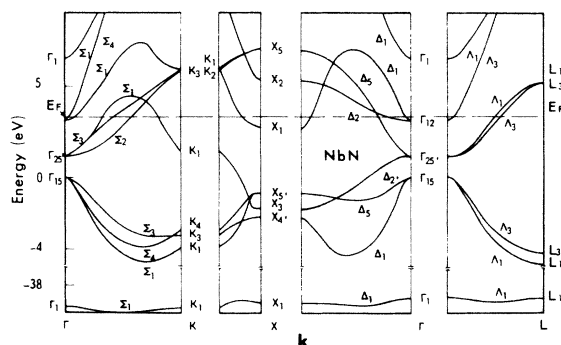


FIG. 2. Electronic energy band structure of NbN. This band structure was obtained from Ref. 5. The zero of energy is at the Γ_{15} level.

calculations.^{3,4,6} The three bands with Γ_{15} symmetry at $\vec{k}=0$ arise mainly from C or N $2p$ states together with some Nb $5p$ states. In addition, there is a small overlap and mixing between these bands and Nb $4d$ states as can be seen in going from Γ to X in the Brillouin zone. This type of overlap is also present in the self-consistent APW calculation of Schwarz⁴ for NbN but is absent in the APW calculation of Mattheiss.³ Some measurements of NbC valence-band x-ray emission spectra^{8,9} indicate that the Nb $4d$ states overlap with the C $2p$ states more than our calculation¹⁰ indicates. To

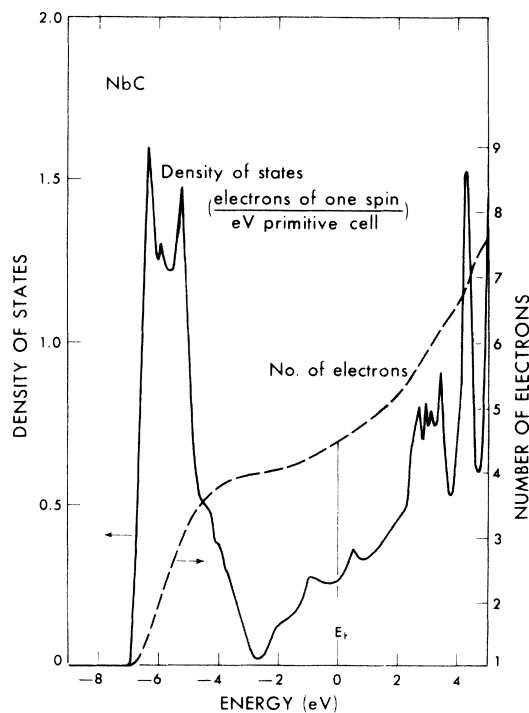


FIG. 3. Density of states of NbC (lowest band not shown) and number of valence electrons per primitive cell volume up to energy E . The number of electrons should be multiplied by 2 for the two possible spin states.

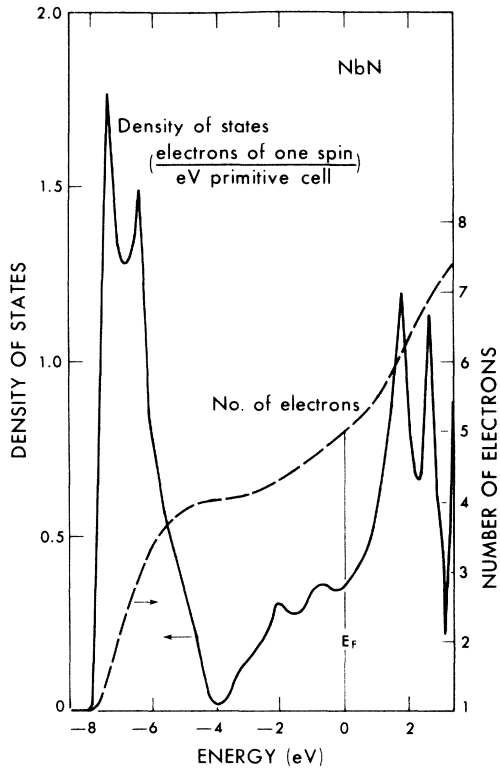


FIG. 4. Density of states of NbN (lowest band not shown) and number of valence electrons per primitive cell volume up to energy E . The number of electrons should be multiplied by 2 for the two possible spin states.

obtain better agreement with these experimental results the C $2p$ states would have to be moved closer to the Fermi energy.

The band structures and band orderings for NbC and NbN shown in Figs. 1 and 2 are seen to be very similar in the region below the Fermi energy E_F . The partially filled bands at E_F come from a mixture of Nb $4d$ states and C or N $2p$ states. The Nb $5s$ state is high in energy and lies above the Fermi energy in both NbC and NbN. The electronic charge in this state has been transferred to the Nb $4d$ levels while some Nb $4d$ -electrons have dropped into the C $2p$ states. The position of the Nb $5s$ level relative to the $5d$ levels is seen to be lower in NbC than in NbN (Figs. 1 and 2). Other calculations on NbN^{3,4} and TiC^{11,12} also reveal the transition metal s states to be above the Fermi energy.

The densities of states $N(E)$ of NbC and NbN (Figs. 3 and 4) are also seen to be very similar. The Fermi energy E_F measured relative to the energy of $\Gamma_{25'}$ state, is higher in NbN than in NbC because of the extra electron in NbN. In both crystals E_F lies in a dip of $N(E)$ and NbN has a larger density of states at E_F than NbC. This could, perhaps, be related to the higher superconducting

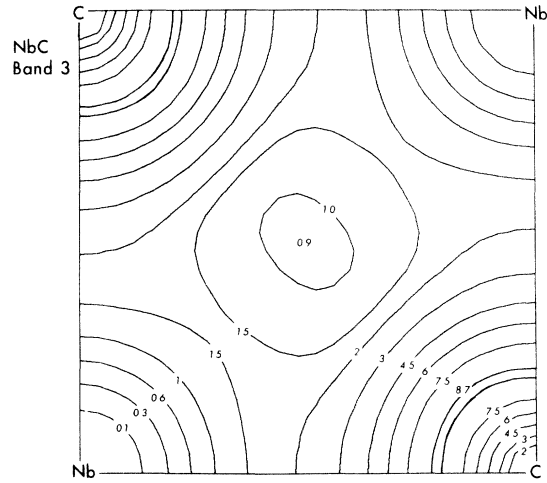


FIG. 5. Electronic charge density of band 3 in the (100) plane of NbC. The charge density arises mainly from C $2p$ states with the Nb $4d$ state making a small contribution. Charge density is normalized to $2e/\Omega$, where Ω is the primitive cell volume.

transition temperature found in NbN. The large peak on the low-energy side of $N(E)$ comes mainly from C or N $2p$ states. The lowest lying C or N $2s$ states are not shown in Figs. 3 and 4.

The charge densities for several bands in NbC and NbN are shown for the (100) and (110) planes in Figs. 5–10. The charge densities for the p -like bands (i. e., bands 2, 3, and 4) are very similar in NbC and NbN. The charge densities of the three bands are also very similar to one another. In Fig. 5 we show the charge density in the (100) plane for one of these bands in NbC. The charge density is p -like

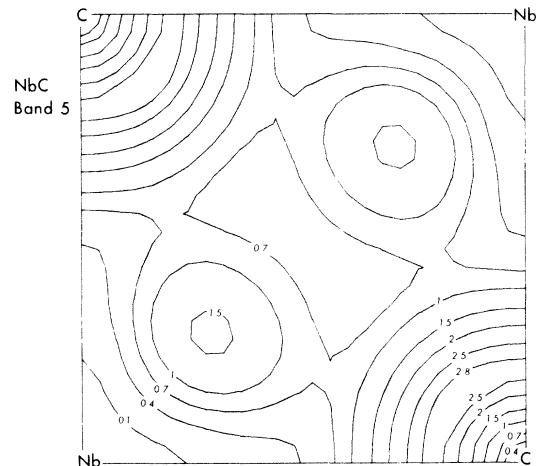


FIG. 6. Charge density of the first partially filled band in NbC for the (100) plane.

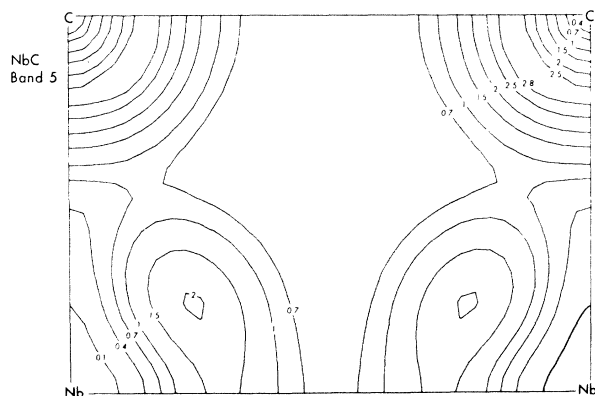


FIG. 7. Charge density of the first partially filled band in NbC for a (110) plane. The "empty" region in the middle with no contours has a nearly uniform charge density of about $0.7 (e/\Omega)$.

around C; it rises to a maximum as we go away from C and then gradually decreases. This is similar to the behavior of the p -like charge densities in semiconductors^{13,14} although the shape of the contours depends on crystal symmetry. The d states of Nb contribute to the small charge density around Nb. The outermost closed contour around C contains approximately 60% of the total charge in band 3 while the corresponding contour around Nb contains only about 15% of the total charge. The remaining 25% of the charge is spread out almost uniformly in the rest of the unit cell.

The higher bands in NbC and NbN are each only partially filled. The first partially filled band (i.e., band 5 with symmetry $\Gamma_{25'}$ at $\vec{k}=0$) contains nearly all the remaining electrons in NbC and over

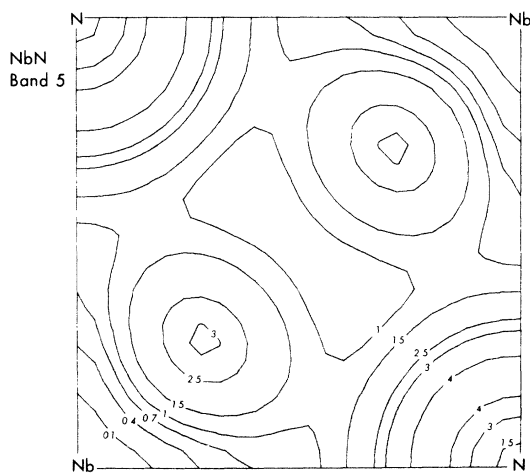


FIG. 8. Charge density of the first partially filled band in NbN for a (100) plane.

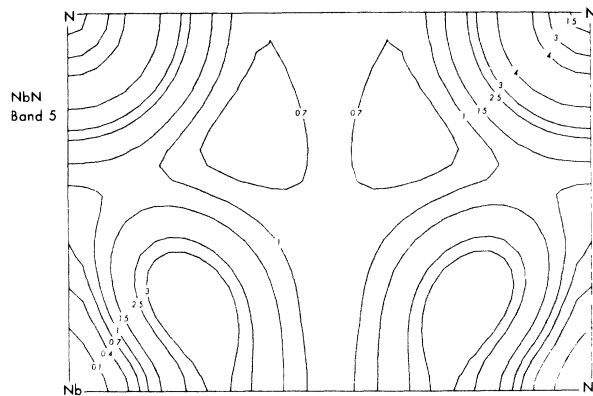


FIG. 9. Charge density of the first partially filled band in NbN for a (110) plane.

80% of the two remaining electrons in NbN. The charge density of this band in the (100) and (110) planes are shown in Figs. 6–9. The interesting feature of these figures are the local maxima in the charge density occurring along the Nb–Nb direction. The magnitude of the charge in the maxima is strongly dependent on the number of electrons per unit cell and is twice as large in NbN (with ten electrons) than in NbC (with nine electrons). These maxima arise from the Nb $4d$ states and have d_{xy} symmetry about the Nb atoms. The charge density of band 5 is not purely d -like; there is a large mixture of C $2p$ states in the wave function which gives the p -like charge distribution around C.

Since the Nb $5s$ state lies above the Fermi energy

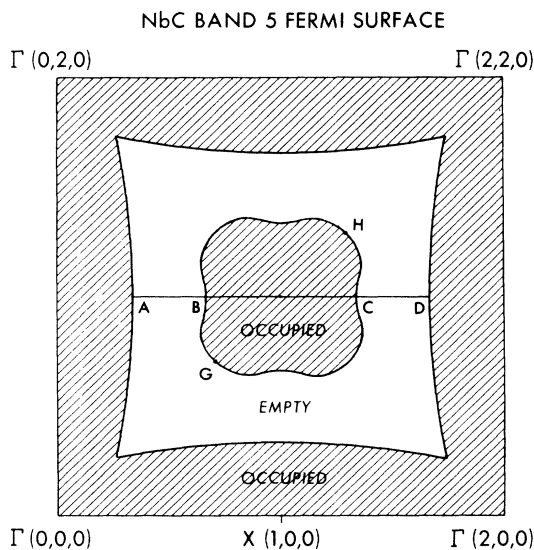


FIG. 10. Cross section of the Fermi surface for the first partially filled band in NbC.

there is no charge localization on Nb; the charge contours around Nb coming from the Nb 4*d* and 5*p* states have much lower values than the combination of *s*, *p* contours around C or N. A spread-out metalliclike charge distribution outside the closed contours around the ions can also be seen in Figs. 5–9. These figures suggest that the bonding in NbC and NbN results mainly from a combination of ionic- and metallic-charge distributions. The C-C, N-N, and Nb-Nb metal and nonmetal nearest-neighbor distances are too large for the formation of localized covalent bonds as in the case of the diamond or zinc-blende crystals where the bonding is characterized by a peak in the magnitude of the charge density on the line joining the nearest-neighbor atoms. The overlap between the bonding orbitals on the ions in NbC and NbN are small and do not produce a maximum in the charge density. The overlap results, instead, in a region, centered halfway between like-atom nearest neighbors, with a slowly varying charge distribution which appears metalliclike. The bonding configuration for NbC and NbN (and probably in other transition-metal compounds as well) can be described as having ionic and covalent-metallic components.

A very interesting property of NbC, NbN, and some other transition-metal carbides is the occurrence of anomalies in the phonon-dispersion curves of those compounds and the association of these with a high superconducting^{15,16} transition temperature, T_c . These phonon anomalies have been interpreted by Weber, Bilz, and Schröder¹⁷ as resulting from resonances in the \vec{q} -dependent polarizability of the metal ions. They attribute the coupling between the metal ions as arising from a charge density with d_{xy} symmetry. This is consistent with the charge density of band 5 in NbC and NbN (Figs. 6–9) which we have obtained. Because of the extra electron in NbN compared to NbC the magnitude of the charge in the d_{xy} peak is larger in NbN than in NbC. The coupling between the Nb atoms is there-

fore expected to be larger in NbN than in NbC. If the number of valence electrons is reduced from 9 to 8 (as in going from NbC to NbC_{0.75}) the magnitude of the charge in the d_{xy} peak becomes nearly zero. It is interesting to note that no phonon anomalies are observed in¹⁵ NbC_{0.75}. If the phonon anomalies and high values of T_c are related to resonances in the \vec{q} -dependent polarizability of the metal ions then it appears that it is band 5 which is most important in determining the superconducting properties of NbC, NbN, and other transition-metal carbides.

A cross section of the Fermi surface of NbC for band 5 is shown in Fig. 10. The Fermi surface of NbN for various bands at the Fermi energy is given in Ref. 5. An interesting feature of the NbC Fermi surface is the magnitude of wave vectors separating the occupied and empty states. The wave vectors *AD* and *BC* (Fig. 10) with $\vec{q} \cong (2\pi/a)(\frac{2}{3}, 0, 0)$ and the wave vector *GH* with $\vec{q} \cong (2\pi/a)(0.5, 0.5, 0)$ are in good agreement with the \vec{q} values at which the anomalies in the phonon-dispersion curves have been observed.¹⁵ It is possible that the shape of the Fermi surface in NbC and NbN can lead to an enhancement of the observed phonon anomalies in these compounds. It should be noted, however, that experimentally the phonon anomalies disappear without any shift in their position when the number of valence electrons is diminished.¹⁵ We expect the shape of the Fermi surface and the wave vectors at which resonance behavior may occur to change with the number of valence electrons.

ACKNOWLEDGMENTS

We would like to thank Dr. Michael Schlüter for a critical reading and discussion of the manuscript. Discussions with J. D. Joannopoulos and Dr. L. Ley are gratefully acknowledged. Part of this work was done under the auspices of the U. S. Atomic Energy Commission.

†Supported in part by National Science Foundation Grant No. GH35688.

¹T. H. Geballe *et al.*, *Physics* **2**, 293 (1966).

²M. L. Cohen and V. Heine, *Solid State Phys.* **24**, 31 (1970).

³L. F. Mattheiss, *Phys. Rev. B* **5**, 315 (1972).

⁴K. Schwarz, *Monatsh. Chem.* **102**, 1400 (1971).

⁵C. Y. Fong and M. L. Cohen, *Phys. Rev. B* **6**, 3633 (1972).

⁶J. B. Conklin, Jr. *et al.*, *J. Phys. (Paris.) Suppl.* **33**, p. C3-213 (1972).

⁷L. A. Hemstreet, C. Y. Fong, and M. L. Cohen, *Phys. Rev. B* **2**, 2054 (1970).

⁸L. Ramqvist *et al.*, *J. Phys. Chem. Solids* **32**, 149 (1971).

⁹J. E. Holliday, *The Electron Microprobe*, edited by T.

D. McKinley, K. S. J. Heinrich, and D. B. Wittry, (Wiley, New York, 1966), p. 3.

¹⁰We became aware of these experimental results after the completion of our calculation.

¹¹J. B. Conklin and D. J. Silversmith, *Int. J. Quantum Chem., Symp.* **2**, 243 (1967).

¹²V. Ern and A. C. Switendick, *Phys. Rev.* **137**, A 1927 (1965).

¹³J. P. Walter and M. L. Cohen, *Phys. Rev. B* **6**, 1877 (1971).

¹⁴M. L. Cohen, *Science* **179**, 1189 (1973).

¹⁵H. G. Smith, *AIP Conf. Proc.* **4**, 321 (1972).

¹⁶H. G. Smith and W. Glaser, *Phys. Rev. Lett.* **25**, 1611 (1970); **29**, 353 (1972).

¹⁷W. Weber, H. Bilz, and U. Schröder, *Phys. Rev. Lett.* **28**, 600 (1972).